

# Topology-mediated approach to the design of quasisymmetric stellarators

E. Rodríguez,<sup>1,2, a)</sup> W. Sengupta,<sup>1,2, b)</sup> and A. Bhattacharjee<sup>1,2, c)</sup>

<sup>1)</sup>*Department of Astrophysical Sciences, Princeton University, Princeton, NJ, 08543*

<sup>2)</sup>*Princeton Plasma Physics Laboratory, Princeton, NJ, 08540*

(Dated: 22 April 2022)

Magnetic confinement fusion designs require careful consideration for them to confine particles effectively. A possible way to do so is to impose *quasisymmetry*. In practice, large-scale optimizations are performed to minimize deviations from exact quasisymmetry. Unfortunately, the large number of parameters and complexity of the optimization process make it challenging to organize and interpret the designs thus obtained. In this Letter, we present a novel topology-mediated description of configurations to describe the space of configurations in a reduced model with a small number of parameters. We show that this approach reproduces existing designs and proves powerful to find potentially attractive new designs, an explicit example of which is presented.

Confining hot plasmas using appropriately shaped magnetic fields is one of the salient problems in plasma physics. A promising confinement concept is the *quasisymmetric stellarator*<sup>1–5</sup>, which has brought about a renaissance in stellarator research. As a subset of *stellarators*<sup>6</sup>, the concept makes use of fully three-dimensional magnetic fields,  $\mathbf{B}$ , but it also includes a form of *hidden symmetry*. *Quasisymmetry* (QS) forces the magnitude  $|\mathbf{B}|$  to be symmetric over flux surfaces<sup>1,7</sup>, even when  $\mathbf{B}$  is not. This leads to excellent confinement of charged particles<sup>1,5</sup> as well as other desirable properties<sup>4</sup>. There are two dominant classes of quasisymmetric configurations. While quasiaxisymmetric (QA) ones have axial symmetry (the long way around the torus axis), quasi-helical (QH) ones have a helical symmetry (with pitch  $\tilde{\alpha}$ ).

In addition to exhibiting QS, a practical quasisymmetric design should preferably be in a state of magnetohydrodynamic (MHD) equilibrium. For fusion plasmas, this involves the balance between the Lorentz force ( $\mathbf{j} \times \mathbf{B}$ , where  $\mathbf{j}$  is the current density) and the gradient of the plasma pressure,  $p$ .<sup>8,9</sup> The conventional approach to obtaining 3D MHD equilibria prescribes the outermost flux surface of the field as a boundary condition and solves the governing equations inside either directly or through a variational approach. In that sense, the description is ‘outside-in’: given a boundary shape, the core (including the centremost degenerate surface: the magnetic axis) emerges as part of the global solution. Quasisymmetric designs are conventionally obtained by choosing those surface shapes that are as close to QS as possible (in the form of an optimization problem)<sup>10,11</sup>. This approach has led to numerous practical designs<sup>11–21</sup>. However, it typically involves a search with a very large number of parameters and does not provide much insight into the structure of quasisymmetric configuration space.<sup>22</sup>

In this Letter, we present a novel approach on quasisymmetric (stellarator-symmetric<sup>23</sup>, vacuum) design, guided by the fundamental idea that the topological properties of the magnetic axis are an excellent point of departure for more efficient identification of stellarators with QS. We propose a reduced model which identifies quasisymmetric configurations with the shape of their magnetic axis and two other shaping parameters for flux surfaces. Our proposed approach may be described as ‘inside-out’ in contrast with the conventional ‘outside-in’ approach discussed above. We demonstrate that this approach reproduces existing designs in a more economical and reduced parameter space and furthermore, elucidates the structure of a ‘phase space’ in which ‘phase transitions’ separate QA and QH designs.<sup>24</sup> In the process, we are able to identify potentially attractive, entirely unexplored regions of designs, discussed below.

The axis and shaping parameters mentioned above emerge naturally from the *near-axis expansion* (NAE)<sup>25–29</sup> of the governing quasisymmetric and equilibrium equations. The NAE is carried out in powers of the distance from the magnetic axis and provides a hierarchy of equations in which the axis and shaping parameters appear as inputs. Our model is obtained by truncating this hierarchy at second order, where deviations from QS first appear in a self-consistent treatment.<sup>26,27</sup> More details regarding the NAE can be found elsewhere.<sup>26–28</sup>

We now discuss the choices of axis and parameters. We start from the zeroth-order in the model, which describes configurations by the shape of the magnetic axis.<sup>24</sup> Identifying configurations with spatially closed curves at the outset endows configuration space with a structure missing in the conventional approach. The space becomes separated into distinct topological regions identified with different forms of QS, which we call *quasisymmetric phases*. Each is associated with a self-linking topological number<sup>30–32</sup>, so that, by continuous deformation, the phase can only change upon crossing a *phase transition* boundary. This corresponds to configurations with axes with curvature vanishing locally, i.e.,  $\kappa = 0$ , at a single or multiple point.

<sup>a)</sup>Email: eduardor@princeton.edu

<sup>b)</sup>Email: wricksg@gmail.com

<sup>c)</sup>Email: amitava@princeton.edu

This newly minted space can be parameterized using a Fourier representation for closed curves (which guarantees curves to be closed<sup>33</sup>). Using cylindrical coordinates, we define the loci of a curve  $(R, Z)$  by  $R = \sum R_n \cos(n\phi)$  and  $Z = \sum Z_n \sin(n\phi)$ . Then the Fourier amplitudes  $\{R_n, Z_n\}$  can be used to represent the space of configurations. The dimensionality of the space will depend on the number of harmonics considered. Most typical quasisymmetric designs belong to a space spanned by two dominant harmonics (with  $R_n \approx Z_n$ )<sup>24</sup>.

At this level, we have identified the space of configurations with spatially closed curves. However, this identification is actually infinitely degenerate; different choices of shaping parameters at higher orders in the NAE represent different configurations. To break the infinite degeneracy at zeroth order, we now move a level up to first order. The model now distinguishes between different elliptically shaped flux surfaces around the axis<sup>25,27,28</sup> as controlled by the choice of the scalar parameter  $\eta$ ,<sup>26,28</sup> which affects both the elongation of the elliptical cross-sections and the rotational transform on axis,  $\iota_0$ .<sup>4</sup> The relation between  $\eta$ , the shaping and the rotational transform is determined primarily by the non-linear *Riccati  $\sigma$ -equation* (see Eq. (2.14) in [27] or Eq. (26) in [28]),

$$\frac{d\sigma}{d\phi} = -\bar{\iota}_0 \left[ 1 + \frac{1}{4} \left( \frac{\eta}{\kappa} \right)^4 + \sigma^2 \right] + \frac{dl}{d\phi} \tau \left( \frac{\eta}{\kappa} \right)^2. \quad (1)$$

where  $\sigma$  is a measure of the tilting and toroidal variation of the elliptical cross section<sup>29</sup>,  $\tau$  is the torsion of the axis and  $dl/d\phi = L/2\pi$ , where  $L$  is the length of the axis. For every magnetic axis shape, Eq. (1) describes a family of configurations spanned by  $\eta$  with different rotational transform  $\bar{\iota}_0 = \bar{\iota}_0(\eta)$ . A convenient choice for  $\eta$  is  $\eta = \eta^*$ , where  $\eta^*$  corresponds to the value of  $\eta$  such that  $d\bar{\iota}_0/d\eta = 0$ . Although this choice might appear at first glance to be arbitrary, it is well-motivated for the following reasons. First, Eq. (1) guarantees its uniqueness for magnetic axes with non-vanishing integrated torsion. Second, in the QA phase, it maximizes the on-axis rotational transform and is everywhere analogous to minimizing the averaged elongation,  $\mathcal{E}$ , of the elliptical flux surfaces  $\langle \mathcal{E}/\kappa^2 \rangle$ . Thus, this choice of  $\eta$  restricts the shaping of surfaces (in the axisymmetric limit giving circular cross-sections) and serves as a form of regularization. With this choice, every point in the optimization space (every axis shape) corresponds to a choice for the elliptical cross-section (through first order).

We now proceed to consider the second-order equations, which bring in the triangular shaping of surfaces, controlled by another scalar parameter  $B_{22}^C$ . This parameter is the symmetric part of the second harmonic magnetic field variation over flux surfaces (more precisely, the variation is given by  $r^2 B_{22}^C$ , where  $r$  is the distance from the axis). However, note that this parameter is not the only source of variation of  $|\mathbf{B}|$  over the surface. At this order there is also a piece of  $|\mathbf{B}|$ , evaluated self-consistently,  $B_{20}(\phi)$ , that generally breaks the symmetry of  $|\mathbf{B}|$ . This formally involves solving (as sketched in

Sec. 4.1 of [27]) a regular second-order ordinary differential equation with periodic boundary conditions and an inhomogeneous term that depends on  $B_{22}^C$  (see Appendix for the explicit equation). Hence, the departure of  $B_{20}$  from a constant represents symmetry-breaking, and  $\Delta B_{20}$  (the difference between the minimum and maximum of  $B_{20}$ ) is a measure of the quality of QS. Together with  $B_{20}$ , several additional relevant features appear at this order in the model, including the shaping of surfaces (and with it the largest attainable aspect ratio<sup>34</sup>), magnetic well properties<sup>35</sup> and magnetic shear<sup>36</sup>. Since our focus is on QS, it is natural to choose the free parameter  $B_{22}^C$  to minimize  $\Delta B_{20}$ . Except in the axisymmetric limit, such a minimum always exists, which serves as the ‘best’ quasisymmetric case.

Further details on the analytic arguments underlying these choices and the structure thereby obtained will be discussed in a separate publication. For the purpose of this Letter, we will explore the effectiveness of this model to assess the quality of quasisymmetric designs in a phase space of configurations with axes described by two dominant harmonic components. This reduced space is shown in Figure 1, constructed for configurations with four field periods. We allow for the  $Z$  component of the axis to differ from  $R$  (generally by a small amount), each point representing the optimal  $Z$  case.

The space in Fig. 1 shows the structure in the form of narrow *branches* of excellent QS and quasisymmetric phases and includes some well-known existing quasisymmetric designs. The phases are separated by phase transitions<sup>24</sup> (see black lines), close to which quasisymmetric designs are generally not practical because they involve very elongated cross-sections. In the QA phase (the phase that includes the origin), there is a dominant branch that grows from the origin in the positive  $a$  direction. This branch does appear to represent many common QA designs correctly. In our perspective, all these designs belong to the same class even though they have important differences, such as the number of field periods. The space in which they are presented here corresponds to  $N = 4$ , but the largely  $N$  invariant features of phase space<sup>24</sup> enable a common qualitative perspective. It is quite remarkable that, given all the room in configuration space accessible to the QA phase, all the QA designs considered seem to be bunched together.

In the QH phase  $\tilde{a}/N = 1$ , we observe two main branches. One which is close to the HSX design<sup>14</sup> (which we shall refer to as the HSX branch) and another that appears not to include any existing design (which we shall refer to as the new QH branch). Other QH designs, especially newly found ones<sup>34</sup>, often live in higher dimensional phase spaces into which these branches extend. The new QH branch is quite remarkable in that no existing design appears to belong to it. This serves as evidence of the power of the current approach, which can be used directly to construct new global equilibria that are approximately quasisymmetric or as a point of departure for further optimization studies. For example, a direct global construc-

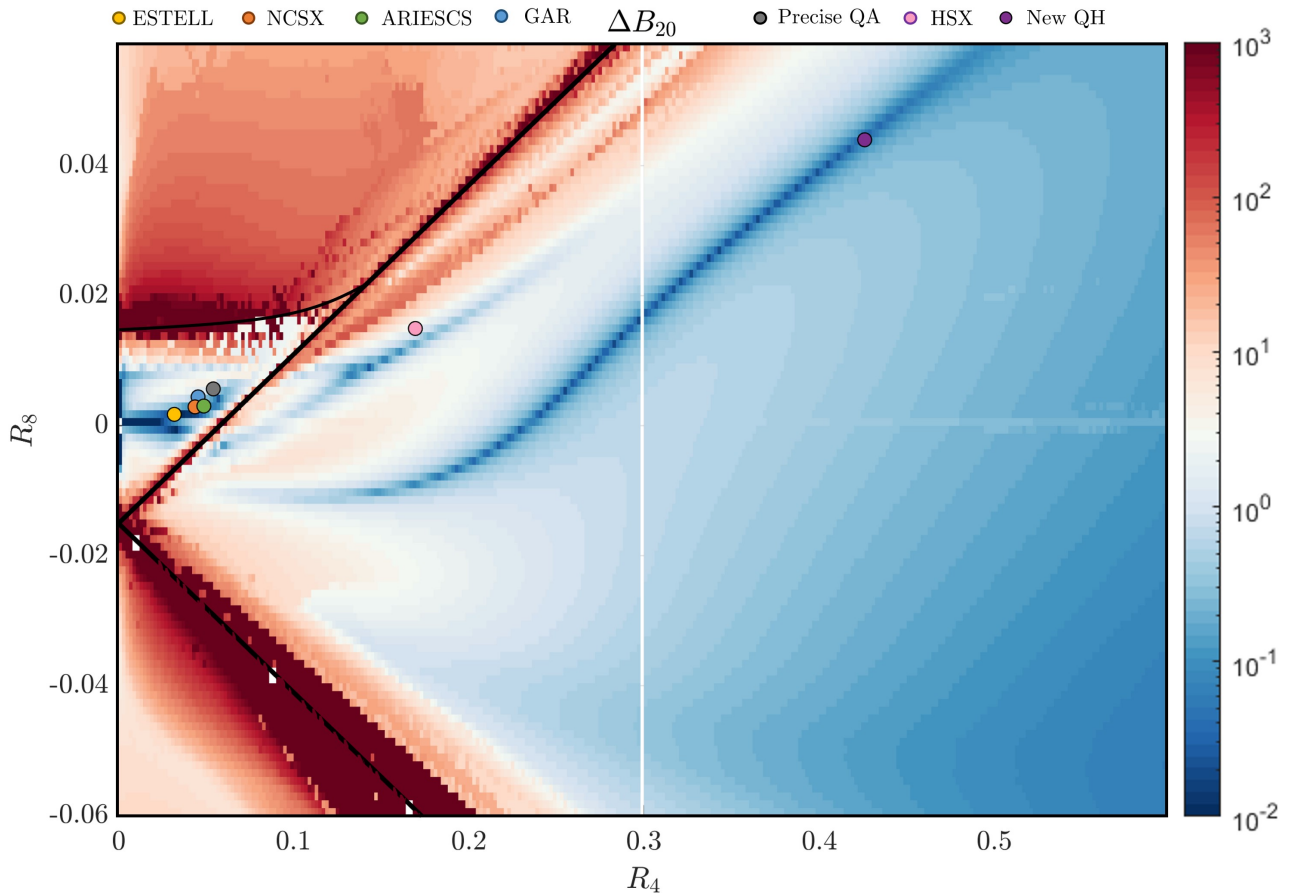


FIG. 1. **Quality of quasisymmetry for the two-harmonic quasisymmetric configuration space.** The figure shows  $\Delta B_{20}$  (in logarithmic scale) for the space of configurations spanned by the two harmonic magnetic axes with four field periods. The  $\{Z_n\}$  harmonics have been, at each point of space, optimized to minimize the quasisymmetry residual. The colored scatter points represent typical quasisymmetric designs in our reduced space (see legend). To represent them all in the same phase space, the magnetic axis harmonics are rescaled as  $R_{4n} = R_{nN}(1 + n^2 N^2)/(1 + 16n^2)$ .<sup>24</sup> The typical designs lie close to the bands of good quasisymmetric quality. The black lines represent phase transition curves for  $R_n = Z_n$ . The dark purple point represents a new QH design, construction of which is presented in Figure 2. The numeric evaluations of the NAE are based on the `pyQSC` code<sup>a</sup>, and cross-checked with a more general code written by the first author.

<sup>a</sup> See <https://github.com/landreman/pyQSC>.

tion may be built by taking the outer surface of the NAE model (with third-order shaping for consistency following Sec. 3 in [27]) and using it as an input to `VMEC`<sup>37</sup>. We present such a configuration, constructed directly from the NAE in Figure 2 corresponding to the point in the new QH branch of Figure 1. We note that although this configuration could, in principle, be stretched up to an aspect ratio of  $\sim 10$  (coming from the limits and shaping at second order), `VMEC` fails to initialize appropriately at aspect ratios significantly smaller than  $\sim 20$ . This numerical difficulty might be one possible explanation for why traditional optimization approaches have missed this class of stellarators.

In summary, we have demonstrated in this paper the power of understanding the space of configurations by an ‘inside-out’ model, which begins from the topologi-

cal structure of the magnetic axis and augments it by a small number of additional parameters (two in our case). Doing so gives this space structure and allows us to explore properties of configurations, including their potential as good quasisymmetric designs. Furthermore, we have explicitly shown that (for  $N = 4$ ) the space of configurations situates existing quasisymmetric designs near predicted branches of potential designs. Finally, the approach, being exhaustive, also allows us to explore new designs, an example of which is given explicitly.

We conclude by thanking R. Jorge for invaluable help with the `pyQSC` and `VMEC` codes, as well as M. Landreman and R. Nies for helpful discussion. This research was supported by a grant from the Simons Foundation/SFARI (560651, AB) and DoE Grant No. DE-AC02-09CH11466. ER was also supported by the Char-

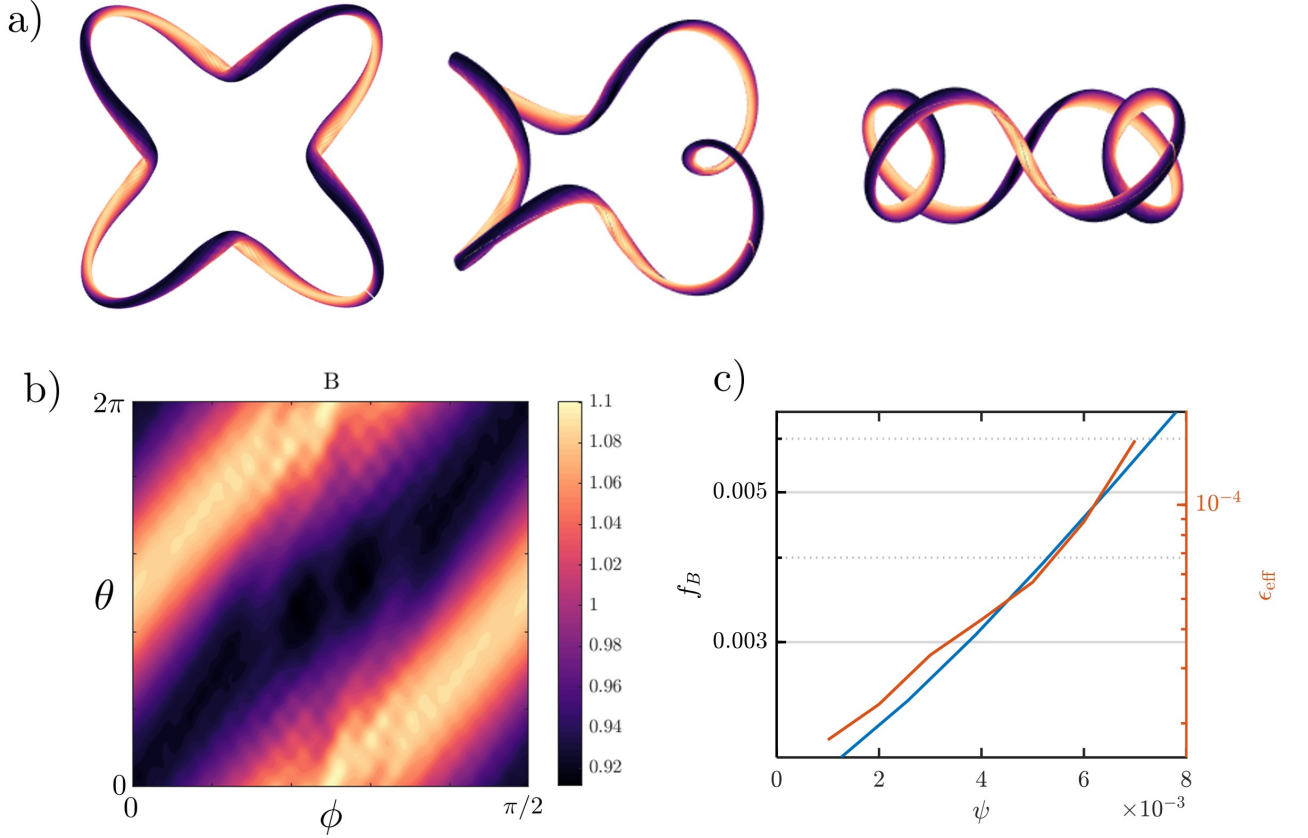


FIG. 2. **Example of new QH branch configuration.** (a) Different projections of the 3D boundary of a configuration from the new QH branch. The colormap represents contours of constant  $|\mathbf{B}|$ . The global equilibria was constructed using VMEC given the surface of a NAE construction with an axis given by the following  $\{R_n, Z_n\}$  components  $R_n = \{0.426, 0.044, -6.36 \times 10^{-11}, 2.85 \times 10^{-5}, 3.89 \times 10^{-8}\}$  and  $Z_n = \{0.411, 0.043, 6.53 \times 10^{-5}, 1.36 \times 10^{-5}, 1.16 \times 10^{-5}\}$ . The higher harmonics have been chosen as small last tweaking choices to further minimize  $\Delta B_{20}$  which within the QS framework we make  $\Delta B_{20} \sim 7 \times 10^{-3}$ . (b) Magnetic field magnitude on the last flux surface of the constructed configuration. (c) Quasisymmetric residual and  $\epsilon_{\text{eff}}$  (measure of particle transport)<sup>38,39</sup> as a function of radius in the global solution showing the quasisymmetric nature of the constructed configuration.

lotte Elizabeth Procter Fellowship at Princeton University.

### Appendix A: Second order ODE on $B_{20}$

The seed of overdetermination at the second-order comes from the magnetic field having to satisfy both the quasisymmetry and equilibrium conditions. The common way to avoid this overdetermination at second order is to relax the condition of quasisymmetry partially. Doing so requires solving a second-order, regular ODE on  $B_{20}$ , the second-order,  $\theta$  independent change in  $1/|\mathbf{B}|^2$ . We write the structure of this equation explicitly here for a stellarator symmetric vacuum. The equation may be written

as,

$$A \frac{d^2}{d\phi^2} \left( \frac{B_{20}}{B_0} \right) + B \frac{d}{d\phi} \left( \frac{B_{20}}{B_0} \right) + C \frac{B_{20}}{B_0} + D = 0, \quad (\text{A1})$$

where,

$$A = -\frac{B_{\alpha 0} \eta}{2\kappa^2 \bar{l}_0} (l')^2 \left[ 1 + \frac{4\kappa^4}{\eta^4 B_{\alpha 0}^2} (1 + \sigma^2) \right], \quad (\text{A2a})$$

$$B = \frac{2B_{\alpha 0} \eta (l')^2}{\bar{l}_0} \frac{\kappa'}{\kappa^3} - \frac{4(l')^2 \sigma}{\bar{l}_0 \eta} \tau, \quad (\text{A2b})$$

$$C = -\frac{1}{2B_{\alpha 0} \eta^3 \kappa^2} \left[ \bar{l}_0 (4\kappa^4 (1 + \sigma^2) - 3B_{\alpha 0}^2 \eta^4) + 8B_{\alpha 0} \eta^2 \kappa^2 \tau \right], \quad (\text{A2c})$$

and  $B_{\alpha 0}^2 B_0 = (dl/d\phi)^2$ . The homogeneous operator only depends on zeroth and first order considerations. How-

ever, the inhomogeneous term  $D$ ,

$$D = \frac{\mathcal{Y}_0^S}{\mathcal{Y}_0^C} \beta_R^C + \mathcal{Y}_1^S \left( \frac{\beta_R^C}{\mathcal{Y}_0^C} \right)' + \beta_R^S, \quad (\text{A3})$$

where,

$$\mathcal{Y}_0^C = \frac{4\bar{l}_0\kappa}{\eta}, \quad (\text{A4a})$$

$$\mathcal{Y}_0^S = \frac{4\kappa' - 8\bar{l}_0\kappa\sigma}{\eta}, \quad (\text{A4b})$$

$$\mathcal{Y}_1^S = -\frac{4\kappa}{\eta} \quad (\text{A4c})$$

$$\begin{aligned} \beta_R^C = \frac{1}{B_{\alpha 0}\eta^3\kappa^2} & \left[ 2B_{\alpha 0}^2\eta^4\kappa^2 (Z_{22}^C - \bar{Z}_{20}) - 6\bar{l}_0\kappa^4\sigma (4\kappa X_{22}^C + \eta^2) + \right. \\ & + 4\kappa^4 (3\bar{l}_0\kappa X_{22}^S + (X_{22}^C\kappa)') \left( \frac{1}{4B_0} \frac{\eta^4}{\kappa^4} + \sigma^2 - 1 \right) + \\ & \left. + 8\kappa^4\sigma (X_{22}^S\kappa)' - 4\kappa^4 \left( \frac{1}{4B_0} \frac{\eta^4}{\kappa^4} + \sigma^2 + 1 \right) (\bar{X}_{20}\kappa)' \right] \quad (\text{A4d}) \end{aligned}$$

$$\begin{aligned} \beta_R^S = \frac{1}{B_{\alpha 0}^2\eta^3\kappa^2} & \left[ 6\bar{l}_0\kappa^4(\eta^2 - 4\kappa\sigma X_{22}^S) + 12\bar{l}_0\kappa^5 \left( \sigma^2 + 1 - \frac{1}{12B_0} \frac{\eta^4}{\kappa^4} \right) \bar{X}_{20} + \right. \\ & + 2B_{\alpha 0}\eta^4\kappa^2 (B_{\alpha 0}Z_{22}^S - \tau) - 8\kappa^4\sigma (X_{22}^C\kappa)' + 2\kappa^4(\eta^2 + 4\kappa\bar{X}_{20})\sigma' + \\ & \left. + 4\kappa^4 \left( \sigma^2 - 1 + \frac{1}{4B_0} \frac{\eta^4}{\kappa^4} \right) ((X_{22}^S\kappa)' - 3\kappa\bar{l}_0 X_{22}^C) \right]. \quad (\text{A4e}) \end{aligned}$$

The various forms of  $X$ ,  $Y$  and  $Z$  needed to complete the expression for  $D$  can be found explicitly in [28] in the simplifying vacuum limit. More explicitly, the forms of  $X$  are found in Eqs. (14)-(15) and Appendix C; the expressions for  $Y$  in Eqs. (27)-(28); and the expressions for  $Z$  in Eq. (24) and following. For a systematic way to obtain these expressions see [36]. This leaves a contribution to  $D$  that is proportional to  $B_{22}^C$ .

- 
- <sup>14</sup>F. S. Anderson, A. F. Almagri, D. T. Anderson, P. G. Matthews, J. N. Talmadge, and J. L. Shohet, *Fusion Technology* **27** (1995).
- <sup>15</sup>M. C. Zarnstorff, L. A. Berry, A. Brooks, E. Fredrickson, G.-Y. Fu, S. Hirshman, S. Hudson, L.-P. Ku, E. Lazarus, D. Mikkelsen, D. Monticello, G. H. Neilson, N. Pomphrey, A. Reiman, D. Spong, D. Strickler, A. Boozer, W. A. Cooper, R. Goldston, R. Hatcher, M. Isaev, C. Kessel, J. Lewandowski, J. F. Lyon, P. Merkel, H. Mynick, B. E. Nelson, C. Nührenberg, M. Redi, W. Reiersen, P. Rutherford, R. Sanchez, J. Schmidt, and R. B. White, *Plasma Physics and Controlled Fusion* **43**, A237 (2001).
- <sup>16</sup>M. Drevlak, F. Brochard, P. Helander, J. Kisslinger, M. Mikhailov, C. Nührenberg, J. Nührenberg, and Y. Turkin, *Contributions to Plasma Physics* **53**, 459 (2013).
- <sup>17</sup>L. Ku and A. Boozer, *Nuclear Fusion* **51**, 013004 (2010).
- <sup>18</sup>F. Najmabadi, A. Raffray, S. Abdel-Khalik, L. Bromberg, L. Crosatti, L. El-Guebaly, P. Garabedian, A. Grossman, D. Henderson, A. Ibrahim, *et al.*, *Fusion Science and Technology* **54**, 655 (2008).
- <sup>19</sup>A. Bader, M. Drevlak, D. T. Anderson, B. J. Faber, C. C. Hegna, K. M. Likin, J. C. Schmitt, and J. N. Talmadge, *Journal of Plasma Physics* **85**, 905850508 (2019).
- <sup>20</sup>S. Henneberg, M. Drevlak, C. Nührenberg, C. Beidler, Y. Turkin, J. Loizu, and P. Helander, *Nuclear Fusion* **59**, 026014 (2019).
- <sup>21</sup>E. J. Paul, T. Antonsen, M. Landreman, and W. A. Cooper, *Journal of Plasma Physics* **86**, 905860103 (2020).
- <sup>22</sup>M. Landreman and A. H. Boozer, *Physics of Plasmas* **23**, 032506 (2016), <https://doi.org/10.1063/1.4943201>.
- <sup>23</sup>R. Dewar and S. Hudson, *Physica D: Nonlinear Phenomena* **112**, 275 (1998), proceedings of the Workshop on Time-Reversal Symmetry in Dynamical Systems.
- <sup>24</sup>E. Rodriguez, W. Sengupta, and A. Bhattacharjee, "Phases

- 
- <sup>1</sup>A. H. Boozer, *The Physics of Fluids* **26**, 496 (1983).
- <sup>2</sup>J. Nührenberg and R. Zille, *Physics Letters A* **129**, 113 (1988).
- <sup>3</sup>M. Tessarotto, J. L. Johnson, R. B. White, and L. Zheng, *Physics of Plasmas* **3**, 2653 (1996).
- <sup>4</sup>P. Helander, *Reports on Progress in Physics* **77**, 087001 (2014).
- <sup>5</sup>E. Rodríguez, P. Helander, and A. Bhattacharjee, *Physics of Plasmas* **27**, 062501 (2020).
- <sup>6</sup>L. Spitzer, *The Physics of Fluids* **1**, 253 (1958).
- <sup>7</sup>E. Rodríguez, W. Sengupta, and A. Bhattacharjee, *Physics of Plasmas* **28**, 092510 (2021).
- <sup>8</sup>M. D. Kruskal and R. M. Kulsrud, *The Physics of Fluids* **1**, 265 (1958).
- <sup>9</sup>R. M. Kulsrud, in *Handbook of Plasma Physics. Basic Plasma Physics 1*, edited by A. A. Galeev and R. N. Sudan (North Holland, Amsterdam, 1983) Chap. 1.4, pp. 1–31.
- <sup>10</sup>E. Rodríguez, E. Paul, and A. Bhattacharjee, *Journal of Plasma Physics* **88**, 905880109 (2022).
- <sup>11</sup>H. E. Mynick, *Physics of Plasmas* **13**, 058102 (2006).
- <sup>12</sup>P. R. Garabedian, *Proceedings of the National Academy of Sciences* **105**, 13716 (2008).
- <sup>13</sup>P. R. Garabedian and G. B. McFadden, *Journal of research of the National Institute of Standards and Technology* **114**, 229 (2009).

- and phase-transitions in quasisymmetric configuration space,” (2022), arXiv:2202.01194 [plasm-ph].
- <sup>25</sup>D. A. Garren and A. H. Boozer, *Physics of Fluids B: Plasma Physics* **3**, 2805 (1991).
- <sup>26</sup>D. A. Garren and A. H. Boozer, *Physics of Fluids B: Plasma Physics* **3**, 2822 (1991).
- <sup>27</sup>M. Landreman and W. Sengupta, *Journal of Plasma Physics* **85**, 815850601 (2019).
- <sup>28</sup>E. Rodríguez and A. Bhattacharjee, *Physics of Plasmas* **28**, 012508 (2021).
- <sup>29</sup>E. Rodríguez and A. Bhattacharjee, *Physics of Plasmas* **28**, 012509 (2021).
- <sup>30</sup>J. Fuller, Edgar J., *The geometric and topological structure of holonomic knots* (1999) p. 112.
- <sup>31</sup>C. Oberti and R. L. Ricca, *Journal of Knot Theory and Its Ramifications* **25**, 1650036 (2016).
- <sup>32</sup>H. K. Moffatt and R. L. Ricca, *Proceedings of the Royal Society of London. Series A: Mathematical and Physical Sciences* **439**, 411 (1992).
- <sup>33</sup>W. Fenchel, *Bulletin of the American Mathematical Society* **57**, 44 (1951).
- <sup>34</sup>M. Landreman, *Journal of Plasma Physics* **87**, 905870112 (2021).
- <sup>35</sup>M. Landreman and R. Jorge, *Journal of Plasma Physics* **86**, 905860510 (2020).
- <sup>36</sup>E. Rodríguez, W. Sengupta, and A. Bhattacharjee, *Physics of Plasmas* **29**, 012507 (2022).
- <sup>37</sup>S. P. Hirshman and J. C. Whitson, *The Physics of Fluids* **26**, 3553 (1983).
- <sup>38</sup>V. V. Nemov, S. V. Kasilov, W. Kernbichler, and M. F. Heyn, *Physics of Plasmas* **6**, 4622 (1999).
- <sup>39</sup>V. V. Nemov, S. V. Kasilov, and W. Kernbichler, *Physics of Plasmas* **21**, 062501 (2014).